Steady-Shear Rheology of Block Copolymer Melts and Concentrated Solutions: Disordering Stress in Body-Centered-Cubic Systems

John M. Sebastian,[†,§] Chiajen Lai[⊥,†] William W. Graessley,[†] and Richard A. Register[*,†,‡]

Department of Chemical Engineering and Princeton Materials Institute, Princeton University, Princeton, New Jersey 08544

Received August 24, 2001; Revised Manuscript Received November 28, 2001

ABSTRACT: We use steady-shear rheology to study the shear-disordering phenomenon in block copolymers in the body-centered-cubic (bcc) mesophase. Polystyrene−polyisoprene and polystyrene−poly(ethylene-*alt*-propylene) diblock, triblock, and starblock systems of varying molecular weight and composition were studied in the melt and as concentrated solutions in a selective solvent. The bcc lattice exhibits a low-frequency modulus G^0_{bcc} which scales with the cube of the lattice spacing and additionally depends only on the proximity to the order−disorder transition (ODT). Steady shear destroys the bcc lattice at a critical shear stress, which is found to be directly proportional to the lattice modulus: $\tau_c = 0.038G^0_{bcc}$ for all block copolymer melts and highly concentrated solutions investigated. The critical stress is thus uniquely determined by the lattice spacing and the proximity to the ODT. The rheological behavior conforms in a remarkably quantitative manner to the shear-melting processes observed in other soft crystalline systems, such as colloidal crystals.

I. Introduction

The ordered mesophase structures in block copolymers endow them with unique and commercially interesting[1] physical properties. The ordered structure also complicates their processing, however, making them the focus of numerous rheological studies over the past few decades.[1−5] Linear viscoelastic measurements have been the primary means for characterizing the rheological response of block copolymers; fewer studies have employed steady-shear techniques.[3−10] Rheology associated with the bcc mesophase has also been less thoroughly examined than for the lamellar or cylindrical mesophases.

The bcc mesophase has commonly been assumed to produce the behavior of a typical viscoelastic solid,[11−17] with a small-strain modulus G^0_{bcc} and a yield stress τ_y below which no flow occurs. Recent investigations suggest, however, that defect-mediated flow mechanisms lead to a more complicated rheology.[3,4,18,19] Indeed, combined scattering and rheological studies of both block copolymer melts[20−22] and micellar cubic crystals composed of block copolymers in selective solvents[23−27] suggest flow mechanisms similar to those found in other materials, ranging from colloidal crystals to metals.

We have recently studied[28] flow in bcc mesophase block copolymer melts, using a combination of small-angle X-ray scattering (SAXS) and steady-shear rheometry. At low deformation rates, these systems remain mesoscopically ordered while manifesting finite although very large Newtonian viscosities ($\eta_0 \approx 10^7-10^8$ Pa·s). This creeping flow is believed to proceed through the motion of defect structures; the specific mechanisms, however, have yet to be identified. A shear-induced disordering process, which destroys the bcc lattice order at a characteristic critical stress, was also demonstrated. Here, we further analyze this shear-melting phenomenon, making quantitative analogies with the flow behavior of other ordered systems (e.g., metals, colloids, and micellar gels). We also describe behavior for a wide range of bcc-forming systems—melts and concentrated solutions of various chemistries, large-scale architectures, and molecular weights—and identify the controlling parameters for this shear-disordering process.

II. Experimental Section

A. Materials. A series of polystyrene−polyisoprene (S/I) block copolymers of various architectures, synthesized via sequential anionic polymerization either by DEXCO Polymers[28−30] or at Princeton,[31] formed the basis for this study. Characterization by gel permeation chromatography (GPC) and ^{1}H NMR spectroscopy is described elsewhere.[28] Some of the polymers synthesized in-house contained detectable terminated S first block and were fractionated in toluene/methanol to yield pure block copolymer (S homopolymer undetectable by GPC, <0.2 wt %) prior to characterization. The diblock and triblock systems all showed monomodal molecular weight distributions with apparent polydispersity indices ($\bar{M}_w/\bar{M}_n$) approaching the resolution of the GPC ($\leq$1.04). The four-arm star S/I-4 10/80 contained approximately 2 wt % coupled material (more than four arms), 11 wt % residual diblock, and 1 wt % residual S first block, which were not removed.

To expand the range of available materials and to investigate any possible influence of chemical structure on the rheology, selective hydrogenation of the I blocks was performed as described previously,[32] yielding their saturated poly(ethylene-*alt*-propylene) derivatives (EP). Hydrogenations were carried out until no unsaturation was detectable by ^{1}H NMR (>99% complete); GPC indicated that no backbone degradation occurred during hydrogenation.

Concentrated solutions were prepared in the I-selective solvent squalane by combining the desired amounts of polymer and squalane and then adding tetrahydrofuran (THF) to accelerate dissolution. Solutions were mixed until homoge-

† Department of Chemical Engineering.
‡ Princeton Materials Institute.
§ Present address: 3M Corporate Research, Science Research Center, St. Paul, MN 55144.
⊥ Present address: Bristol-Myers Squibb Pharmaceutical Research Institute, P.O. Box 191, New Brunswick, NJ 08903.
* To whom correspondence should be addressed. E-mail register@princeton.edu, tel (609) 258-4691.

10.1021/ma011523+ CCC: $22.00
Published on Web 02/21/2002

Table 1. Characteristics of Block Copolymer Materials Studied

polymer code[a]	sample description[b]	wt % styrene[c]	mol wt (kg/mol) $\bar{M}_n$	mol wt (kg/mol) $\bar{M}_w$	T_{ODT} (°C) as determined by rheology	T_{ODT} (°C) as determined by SAXS
S/I 7/46	diblock melt	13.0	51.5	52.9	110 ± 2	111 ± 2
S/I 9/57	diblock melt	13.5	64.3	65.9	156 ± 2	161 ± 2
S/I 10/57	diblock melt	15.3	64.7	67.0	nd[d]	225 ± 2
S/I 60/7	diblock melt	89.0	64.9	67.7	165 ± 2	165 ± 2
S/I 10/69	diblock melt	13.1	76.7	79.0	197 ± 2	202 ± 2
S/I/S 9/120/9	triblock melt	13.0	133	138	164 ± 2	167 ± 2
S/EP 3/24	diblock melt	12.4	26.4	27.1	nd	121 ± 2
S/EP 5/36	diblock melt	12.9	40.1	41.7	242 ± 2	249 ± 2
S/EP/S 5/67/5	triblock melt	11.9	87.9	92.3	266 ± 2	272 ± 2
S/I 12/10:25	diblock solution, 24.9 wt % polymer	51.6 (13.0)	21.9	22.6	nd	131 ± 2
S/I 12/10:30	diblock solution, 30.0 wt % polymer	51.6 (15.6)	21.9	22.6	146 ± 2	142 ± 2
S/I 12/10:40	diblock solution, 40.0 wt % polymer	51.6 (20.8)	21.9	22.6	155 ± 2	158 ± 2
S/I 8/17:39	diblock solution, 38.8 wt % polymer	33.4 (13.0)	24.3	25.2	nd	123 ± 2
S/I 10/69:23	diblock solution, 23.2 wt % polymer	13.1 (3.0)	76.7	79	nd	111 ± 2
S/I/S 9/120/9:23	triblock solution, 23.1 wt % polymer	13.0 (3.0)	133	138	nd	102 ± 2
S/I-4 10/80:23	4-arm star block solution, 23.0 wt % polymer	11.6 (2.7)	341	357	nd	115 ± 3

[a] Values in parentheses indicate the polymer weight percent in solution. [b] All solutions are prepared in the I selective solvent squalane. [c] Values in parentheses indicate the total S weight percent in solution. [d] nd = not determined by this method.

neous and then placed under flowing N_2 at room temperature. When less than 10 wt % THF remained, the solutions were slowly heated to 70−80 °C under vacuum until all THF was removed. The solutions were transparent and showed no evidence of phase separation or syneresis even after several months. Because the vapor pressure of squalane is very low (0.05 mmHg at 176 °C), virtually no squalane evaporates during solution preparation or rheological testing, even at 150 °C for 3−5 days.

Table 1 summarizes the characteristics of the materials studied. Bulk materials are coded as S/A *m*/*n*, where A is either I (isoprene) or EP and *m* and *n* are the approximate $\bar{M}_w$ values of the S and A blocks in kg/mol. Concentrated solutions are coded as S/A *m*/*n*:*w*, where *w* is the weight percent of polymer in the solution.

B. Rheological Measurements. Rheological testing was performed using a dynamic stress rheometer (DSR-200, Rheometric Scientific), as described in detail in the companion paper.[28] Test specimens were prepared by compression molding under vacuum into disks: bulk diblocks were molded at room temperature, triblock and starblock solutions at 55 °C, and bulk triblocks at 120 °C. Diblock solutions were simply spread onto the rheometer's lower plate. After loading in the rheometer, to ensure that the equilibrium morphology was attained, samples were heated to at least 5 °C above T_{ODT} for 15 min and then quenched to the desired testing temperature, and the dynamic moduli were monitored at $\omega \approx 10^{-2}$ rad/s until both moduli attained their limiting values.[30] All experiments were conducted under a continuous N_2 purge; specimens examined by GPC after rheological testing showed little (<10%) to no indication of degradation even after testing at 150 °C for 3−5 days. All measurements were conducted above the glass transition temperature of the polystyrene microdomains.

C. Small-Angle X-ray Scattering Measurements. SAXS data were collected as described elsewhere[28,30] and are presented as absolute intensity vs scattering vector $q = (4\pi/\lambda) \sin\theta$, where λ is the radiation wavelength and 2θ is the scattering angle. Measurements were made at elevated temperatures using a hot stage controlled to ±1 °C by a microprocessor-controlled resistive heater.[30] Bulk block copolymers were run under vacuum, while concentrated solutions were run under a slow flow of He at atmospheric pressure to limit evaporation of the solvent. SAXS confirmed that each system exhibited a bcc lattice structure when ordered and also yielded the order−disorder transition temperature (T_{ODT}), confirmed for several systems via rheology.[29,30]

III. Results

A. Linear Viscoelastic Behavior. At low deformation rates the linear viscoelastic response of bcc phase

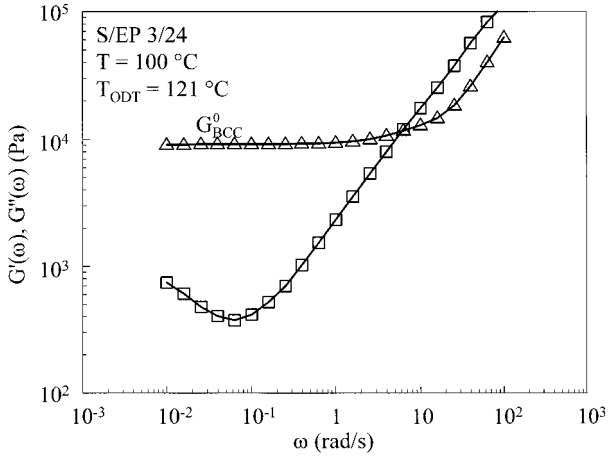

Figure 1. Dynamic frequency sweep for the ordered diblock S/EP 3/24 at 100 °C, illustrating the bcc lattice modulus G^0_{bcc} observed at moderately low frequencies. (□) $G''(\omega)$; (△) $G'(\omega)$.

block copolymer systems should ideally be that of a three-dimensional crystalline solid,[2−4,18] with a characteristic modulus G^0_{bcc}. The dependence of G^0_{bcc} on the interparticle spacing *r* should be of the general form[33]

$$G^0_{bcc} \sim \frac{1}{r_0}\left[\frac{\partial^2 U(r)}{\partial r^2}\right]_{r_0} \qquad (1)$$

where $U(r)$ is the interparticle potential and r_0 is the equilibrium intersphere spacing. For bcc-forming block copolymer systems, $U(r)$ has not been definitively established. The typical relation employed for hard-sphere systems scales $U(r) \sim k_BT/r^n$ (*n* typically 5−20), while for soft spheres the potential is better represented as $U(r) \sim k_BT \ln(1/r)$, where k_B is Boltzmann's constant and *T* is absolute temperature.[34−36] In either case, it is thus presumed from eq 1 that the modulus should scale as $G^0_{bcc} \sim k_BT/r_0{}^a$. Indeed, a best-fit value of $a = 3.14$ was found in a study of bcc-forming block copolymer melts.[18]

For each of the block copolymer systems used in this study, dynamic frequency sweeps (DFS) yielded results such as those shown in Figure 1; the numerical value of G^0_{bcc} was obtained from the DFS by averaging the values of G' over the region which showed very little frequency dependence, in the vicinity of the minimum

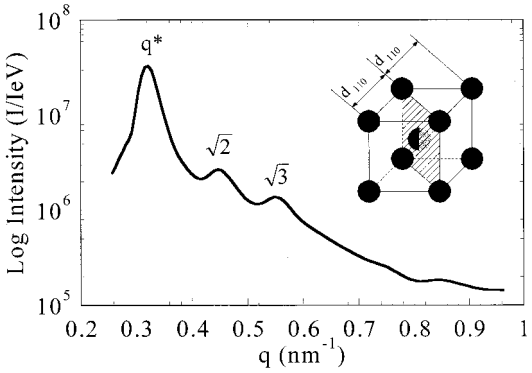

Figure 2. SAXS pattern for the ordered diblock S/EP 3/24 at 100 °C, revealing peaks in q/q^* ratios of 1:√2:√3, characteristic of the bcc lattice. The inset is a schematic showing the characteristic lattice spacing d_{110} (= $2\pi/q^*$).

Table 2. Microstructural and Rheological Characteristics of Block Copolymer Melts and Solutions

polymer code [T_{ODT}, in °C]	temp (°C)	d_{110} (nm)	G^0_{bcc}(Pa)	τ_c (Pa)
S/I 7/46 [110 °C]	90	24.1	5760	220
	100	24.0	4950	190
S/I 9/57 [156 °C]	105	27.2	5680	220
	140	26.7	4490	175
	150	26.4	3890	nd[a]
S/I 10/57 [225 °C]	120	29.9	6850	230
	140	30.2	5700	225
S/I 60/7 [165 °C]	140	24.3	6300	250
S/I 10/69 [197 °C]	125	29.8	5000	200
	140	29.8	4800	200
	155	29.7	4510	175
	170	29.4	4330	150
	185	29.0	3560	135
S/I/S 9/120/9 [164 °C]	120	28.1	4770	210
	130	28.2	4600	190
	140	28.1	4330	175
	155	27.6	3640	120
S/EP 3/24 [121 °C]	100	19.6	9580	360
	110	19.5	8560	300
S/EP 5/36 [242 °C]	140	24.5	8780	360
	180	24.9	8220	330
S/EP/S 5/67/5 [266 °C]	200	27.8	5770	210
S/I 12/10:25 [131 °C]	85	26.8	3400	35
S/I 12/10:30 [146 °C]	120	24.1	6940	195
	135	23.1	5800	150
S/I 12/10:40 [155 °C]	140	21.6	9500	300
S/I 8/17:39 [123 °C]	105	23.1	7000	235
	120	22.4	5600	nd
S/I 10/69:23 [111 °C]	65	37.3	1740	64
S/I/S 9/120/9:23 [102 °C]	85	36.1	1825	67
S/I-4 10/80:23 [115 °C]	90	39.2	1350	55
	100	39.2	1320	50

[a] nd = not determined.

in G''. For bcc systems, the spacing d_{110} between (110) planes may be determined from SAXS as $d_{110} = 2\pi/q^*$, where q^* is the position of the primary peak. (A bcc lattice will also manifest a series of higher-order SAXS peaks having q/q^* ratios of 1:√2:√3, as shown in Figure 2.) The values of G^0_{bcc} and d_{110} for each system at various temperatures are listed in Table 2.

The free energy of a block copolymer system, and hence $U(r)$, depends on the segregation strength of the system χN, where χ is the Flory−Huggins interaction parameter between the monomer residues forming the two blocks and N is the degree of polymerization. Therefore, to compare the $G^0_{bcc}-d_{110}$ relations for different systems, they should all be at the same reduced

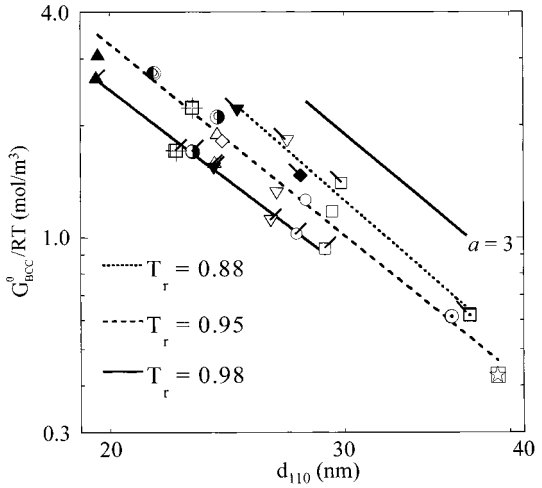

Figure 3. Lattice modulus G^0_{bcc}/RT as a function of the lattice spacing d_{110} for various systems at a reduced temperatures $T_r = T/T_{ODT}$ of 0.88, 0.95, and 0.98. The lines passing through the data are power-law fits having exponents of −3.13, −2.90, and −2.72, respectively. Systems are S/I 7/46 (△), S/I 9/57 (▽), S/I 60/7 (◇), S/I 10/69 (□), S/I/S 9/120/9 (○), S/EP 3/24 (▲), S/EP 5/36 (▼), S/EP/S 5/67/5 (◆), S/I 12/10:30 (◑), S/I 12/10:40 (◐), S/I 8/17:39 (⊞), S/I 10/69:23 (⊡), S/I/S 9/120/9:23 (⊙), S/I-4 10/80:23 (☆). Symbols representing data taken at T_r = 0.88 are further decorated with a backslash (\); at T_r = 0.98, with a foreslash (/). Solid line with a slope of −3 is shown to the right of the data for comparison.

segregation strength $\chi N/(\chi N)_{ODT}$. However, determining the precise temperature dependence of χ is much more difficult than determining its approximate magnitude, and different researchers have reported significantly different temperature dependences for the same system.[29] Moreover, for the block copolymer solutions in squalane, even the magnitude of χ is difficult to assess, as there are multiple interactions present (i.e., block−block and block−solvent). Therefore, we take a pragmatic approach[18] and instead compare systems at the same reduced temperature $T_r \equiv T/T_{ODT}$, with T in absolute units.

Figure 3 shows a log−log plot of G^0_{bcc}/RT vs d_{110} for various systems at T_r = 0.88, 0.95, and 0.98 ± 0.01. The polymers described by these data cover a wide range of molecular weight and composition, various architectures, and block chemistries and include both melts and concentrated solutions, yet the same $G^0_{bcc}-d_{110}$ scaling holds at a given T_r to within experimental error. The scaling exponents (±1 standard deviation of the fit) were found to be a = 3.13 ± 0.26, 2.90 ± 0.12, and 2.72 ± 0.13 at T_r = 0.88, 0.95, and 0.98, respectively. The near constancy of a is evident in the near parallelism of the three curves in Figure 3, and indeed, the slope for each line is close to 3. This result is intuitively appealing as it implies that the modulus is proportional to the number density of spheres, with each sphere per unit volume contributing a certain multiple of k_BT to the modulus at each reduced temperature, independent of the size of the sphere. Note that this result differs from the expectation of Watanabe et al.,[37] who proposed that each chain per unit volume should contribute k_BT to the modulus in micellar block copolymer solutions; the number of chains per sphere varies substantially with both d_{110} and system chemistry for the data shown in Figure 3.

The value a = 3 implies a potential, through eq 1, of the form $U(r) \sim k_BT \ln(1/r)$. This form is similar but not

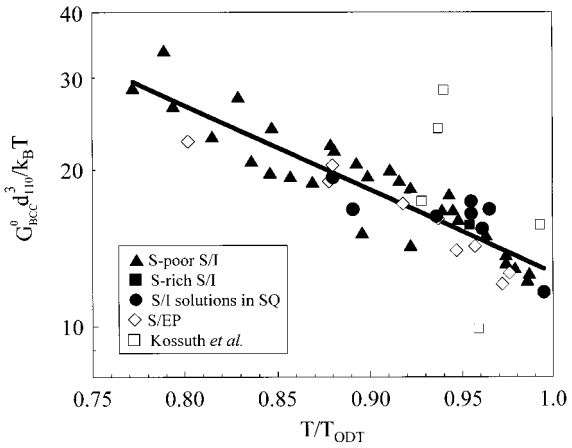

Figure 4. Reduced lattice modulus $G^0_{bcc}d_{110}{}^3/k_BT$ vs reduced temperature $T_r \equiv T/T_{ODT}$, for all materials in Table 2 save the S/I 12/10 solutions. Solid line is the best-fit exponential expression (eq 3). Materials are grouped into four broad categories: all polystyrene-poor S/I and S/I/S melts (▲); the polystyrene-rich S/I 60/7 melt (■); concentrated S/I diblock, triblock and starblock solutions in squalane (●); S/EP and S/EP/S melts (◇). The melt data of Kossuth et al.[18] (□) are plotted for comparison but not included in the fit.

identical to that proposed by Witten and Pincus[38] for spheres with interacting grafted polymer layers: $U(r) \sim f^{3/2}k_BT\ \ln(1/r)$, where f is the number of grafted polymer chains per sphere (for the diblock case, the sphere aggregation number[39]). This additional factor of $f^{3/2}$ is thus predicted to also appear in G^0_{bcc}, through eq 1. In fact, f varies substantially across Figure 4, such that the superposition is much poorer if the modulus is divided through by $f^{3/2}$, so the simpler form of the potential (with no explicit dependence on f) seems to best describe our results.

The temperature dependence of the reduced modulus is clearly revealed by plotting $G^0_{bcc}/d^3_{110}k_BT$ against T_r in Figure 4. All our data lie within a ±22% band of a simple exponential dependence, shown as the solid line:

$$G^0_{bcc}d^3_{110}/k_BT = 12.7\ \exp[-3.70(T_r - 1)] \qquad (2)$$

The data of Kossuth et al.,[18] shown in Figure 4 as well, scatter about eq 2 though they were not included in the fit. For the bcc lattice, there is one sphere per $\sqrt{2}d^3_{110}$, so according to eq 2, right at the ODT ($T_r = 1$) each sphere per unit volume contributes $18k_BT$ to the modulus. Alternatively, each of the pairwise interactions between the eight nearest neighbors in the bcc structure contributes $4.5k_BT$ per unit volume to the modulus. We note that the successful generation of a master curve scaled on T_r shows post facto that T_r is an adequate surrogate for the reduced segregation strength, at least over the limited range of T_r employed in Figure 4.

B. Steady-Shear Behavior. The steady-shear behavior of the spherical phase is one of the least well-studied aspects of block copolymer rheology.[3−5] In the companion paper,[28] we employed creep testing to generate flow curves such as that depicted in Figure 5 for the diblock S/EP 3/24 at 100 °C. As can be seen from the double-logarithmic plot of η vs τ, there are three distinct flow regimes characteristic of the steady-shear rheology of ordered bcc block copolymers; the microstructural order present in each of the three regimes was determined by SAXS measurements.[28] In the low-stress regime, the flow behavior is characterized by a

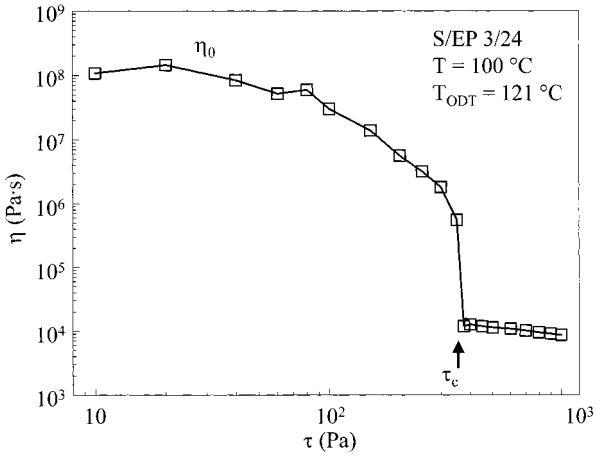

Figure 5. Flow curve for the ordered diblock S/EP 3/24 at 100 °C, showing η_0 characteristic of the low-stress regime and τ_c characteristic of the transition regime.

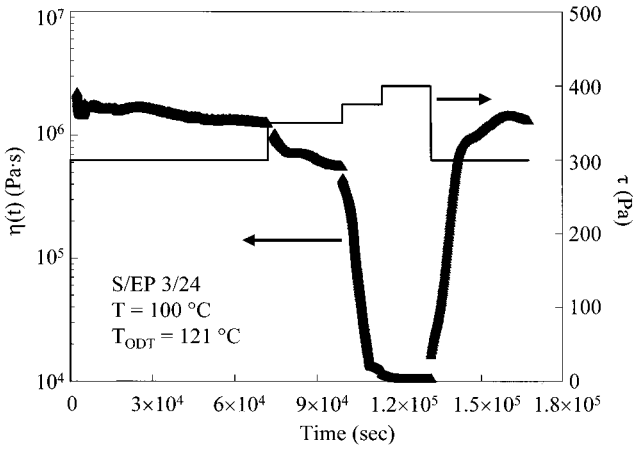

Figure 6. Temporal progression of $\eta(t)$ for S/EP 3/24 at 100 °C (symbols forming thick solid line) with incremental increases in applied τ (thin solid line), demonstrating the drastic change in flow behavior occurring at τ_c.

Newtonian viscosity η_0 yet the bcc lattice is still present, suggesting that defect-mediated relaxations occur which permit steady creep in the ordered state. In the transition regime, η drops by 3−4 orders of magnitude with an increase in τ of only a factor of 3, as shear disordering of the bcc lattice occurs; for $\tau > \tau_c$, the system's microstructure is equivalent to that obtained by thermally disordering these materials via a quench from $T > T_{ODT}$. Finally, in the high-stress regime, the flow behavior is that of a weakly shear-thinning polymeric material because there is no lattice structure present.[28] We now address the issue of what sets the value of the critical stress τ_c and compare the shear-disordering process in our block copolymer materials with similar behavior in other soft crystalline systems.

In Figure 6, the time evolution of η is shown for S/EP 3/24 at 100 °C as τ is stepped incrementally from 300 to 400 Pa, corresponding to stresses within the flow transition regime (Figure 5). When τ is increased from 300 to 350 Pa, η drops by roughly a factor of 2, from 1.3×10^6 to 5.7×10^5 Pa·s. The drop in η is not instantaneous when τ is increased; η falls off progressively, presumably reflecting a gradual increase in the fraction of disordered material, and eventually levels out at a new value which is stable indefinitely. When τ is increased from 350 to 370 Pa, there is a much larger change in the flow behavior, η falling by more than a

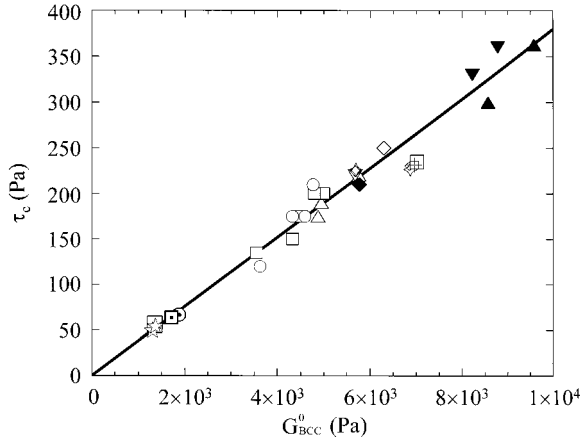

Figure 7. Plot of τ_c vs G^0_{bcc} for all of the systems listed in Table 2 save the S/I 12/10 solutions. The solid line has a best-fit slope of 0.038. Symbols are the same as in Figure 3.

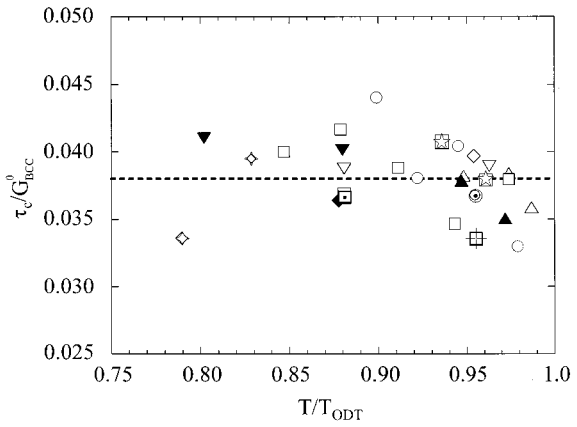

Figure 8. Plot of τ_c/G^0_{bcc} vs T/T_{ODT} ($\equiv T_r$) indicating no clear correlation. The dashed line indicates the average value obtained from the fit in Figure 7; symbols are the same as in Figure 3.

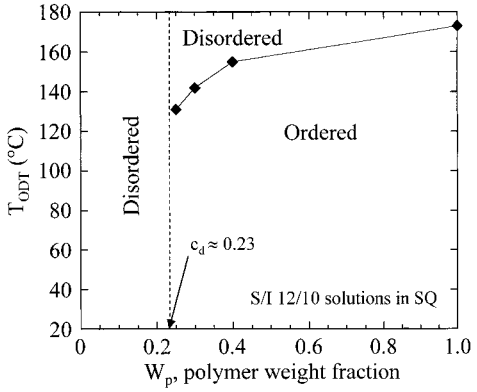

Figure 9. Dependence of T_{ODT} on polymer concentration for S/I 12/10 solutions in squalane, demonstrating the critical disordering concentration c_d at 0.23 polymer weight fraction.

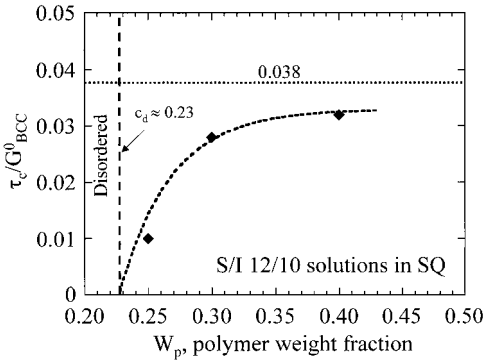

Figure 10. Dependence of τ_c/G^0_{bcc} on polymer concentration for diblock S/I 12/10 solutions in squalane showing a drop in this ratio from the average value (0.038) as c_d (0.23 polymer weight fraction) is approached. The hatched line describing the data points is drawn as a guide to the eye.

factor of 50 to 1×10^4 Pa·s; we assign τ_c as the point of steepest decline, 360 ±10 Pa. Usually τ_c occurs at the "foot" of the precipitous drop in η vs τ, at which point the bcc lattice is also completely eradicated. When τ is further increased from 370 to 400 Pa, η decreases only slightly; the shear-disordered state behaves as a simple shear-thinning material with no further microstructural changes occurring. However, if now τ is decreased below τ_c (to 300 Pa in Figure 6), η eventually returns to its original level (1.3×10^6 Pa·s) as the system redevelops its bcc structure. We have shown that the kinetics of the reordering process following shear disordering are equivalent to those following a quench from above the order−disorder transition temperature.[28]

Measurements of τ_c were made at various temperatures for each of the block copolymer systems listed in Table 1. The values, listed in Table 2, are plotted in Figure 7 against the values of G^0_{bcc} for each of the melts and concentrated solutions, excluding the concentrated solutions of S/I 12/10 discussed below. A straight line through the origin accommodates the data for all systems examined:

$$\tau_c = 0.038 G^0_{bcc} \tag{3}$$

with a standard deviation of only 0.001 in the proportionality constant. This result implies that the lattice disorders once a critical shear strain (0.038) is reached; the temperature dependence of τ_c is entirely given by the temperature dependence of G^0_{bcc}, already described in the previous section. A critical test of this idea is given in Figure 8, where τ_c/G^0_{bcc} is plotted against T_r for all the data in Figure 7. Any temperature dependence of τ_c/G^0_{bcc} is slight at best.

However, for block copolymer solutions, changes in critical strain become evident as the polymer content is reduced. As shown in Figure 9, concentrated solutions of the diblock S/I 12/10 in squalane form the bcc structure at low temperatures and disorder at higher temperatures; T_{ODT} changes only modestly with dilution over most of the concentration range. However, when the system is diluted from 25 to 22.5 wt % polymer, the solution goes from having a bcc structure with T_{ODT} = 131 °C to being disordered over the entire temperature range (T_{ODT} < 75 °C, the glass transition temperature of the S-rich spheres[31]). Below this critical concentration c_d (≈23 wt % polymer), the corona (I) blocks can no longer maintain a uniform concentration profile within the mesophase matrix, and the lattice structure is lost. Figure 10 shows the corresponding values of τ_c/G^0_{bcc} at concentrations slightly above c_d. As the polymer concentration is reduced toward c_d, the value of τ_c/G^0_{bcc} decreases correspondingly. We conclude that the lattice becomes weaker as c_d is approached because dilution reduces the interactions between the coronae of adjacent micelles.[12] Similar findings were obtained by Kelarkis et al.[40] for aqueous solutions of two poly(ethylene oxide)−poly(butylene oxide) diblocks: at higher concen-

trations, a "hard" fcc gel is formed (with $\tau_y/G'(1\text{ Hz}) = 0.029$), but as the copolymer is further diluted, both the lattice structure and the yield stress disappear.

IV. Discussion

The theoretical shear strength τ_{max} in perfect crystalline systems is the stress required to cause a layer of particles to hop from their original lattice sites into adjacent sites. Frenkel[41] did the first calculation for τ_{max}, obtaining

$$\tau_{max} = \frac{Gd}{2\pi h} \tag{4}$$

where d is the repeat distance in the shear direction and h is the interplanar spacing. With $d \approx h$, $\tau_{max}/G \approx {}^1/_{2\pi} \approx 0.16$. Frenkel's prediction is equivalent to considering only the first two terms in a Fourier series of the potential energy variation with particle displacement $U(r)$. When additional terms are included, τ_{max}/G is predicted to fall between 0.02 and 0.04 for many fcc metals.[42] For most bcc metals,[42] this ratio is estimated to be 0.10, but for elastically anisotropic systems such as sodium, models[43] for shear of {110} planes in ⟨110⟩ directions predict $\tau_{max}/G = 0.036$; shear of the {110} planes in ⟨111⟩ directions, the preferred slip system for bcc-forming block copolymers,[20,21] is thus predicted[42] to occur at $\tau_{max}/G = 0.02$.

In bcc block copolymer systems, τ_c may be considered analogous to τ_{max} despite the flow at values of $\tau < \tau_c$. We presume this creeping motion is mediated by defects, and indeed, even polycrystalline metals and ceramics exhibit Newtonian creep at elevated temperatures.[44−46] But compared with atomic crystals, where interparticle forces are strongly attractive and keep the bulk system ordered even at $\tau > \tau_{max}$, the restoring force in soft materials is weak. If the particles are displaced significantly from their equilibrium positions, they do not quickly return to lattice sites, and so the system shear melts. The sluggish ordering kinetics of highly asymmetric block copolymers[28,30] are consistent with the idea that the lattice, when disrupted, does not redevelop rapidly.

Our results for the shear-disordering process in sphere-forming block copolymers, as embodied in Figure 7, led us to reexamine previous work. A pioneering study by Hashimoto and co-workers[14] examined concentrated solutions of polystyrene−polybutadiene (S/B) diblocks in the selective solvent *n*-tetradecane, similar to our concentrated solutions in squalane. From SAXS, the authors discerned that the micelles were ordered onto a cubic lattice, and from controlled-strain-rate rheometry, they inferred that these systems showed a true yield stress τ_y (extrapolated from measurements at higher deformation rates) above which the lattice structure is destroyed,[14] which we identify with our τ_c. Dividing by the low-frequency modulus measured for each solution (denoted G_0, should be similar to G^0_{bcc}), we obtain τ_y/G_0 values ranging from 0.02 to 0.06 that increase monotonically with polymer concentration. These results bracket our value of $\tau_c/G^0_{bcc} = 0.038$; the reduction in τ_y/G_0 with reduced polymer concentration is also reminiscent of our results shown in Figure 10.

Eiser et al. have recently reported extensive studies on a concentrated aqueous solution of a poly(ethylene oxide)−poly(propylene oxide)−poly(ethylene oxide) triblock exhibiting the bcc structure.[47,48] They observed two abrupt drops in viscosity at closely spaced stresses (<3% difference); these stress values also correspond to approximately 4% of the lattice modulus, though the linear viscoelastic data for this polyoxide solution do not show as clear a G^0_{bcc} plateau as (for example) Figure 1. From complementary SAXS measurements, Eiser et al. concluded that the viscosity drops resulted from a transformation of the initially polygrain sample to first one highly oriented structure and then to another, rather than from a complete destruction of the lattice as we observe. This polyoxide solution has a significantly smaller lattice spacing, and much faster lattice dynamics, than any of the block copolymer materials we have studied; indeed, the onset of terminal behavior is evident at $\omega < 0.2$ rad/s in the polyoxide solution (compare Figure 1). A hypothesis for the difference is thus that the initial viscosity drop observed in the polyoxide solution does reflect a partial disordering of the lattice but that this solution can "reorder" during flow, in a favorable orientation.

In colloidal crystals, similar shear-induced melting behavior has been reported[49−53] with values for τ_c/G (0.03−0.05) similar to ours, perhaps indicating an underlying commonality in rheological mechanism. For example, studies of colloidal crystals composed of charge-stabilized silica spheres show a steady flow at low deformation rates while retaining crystalline order.[49] At higher rates a shear-melting transition occurs, progressively transforming the three-dimensional lattice into a disordered liquid structure beyond a critical stress τ_c proportional to the modulus ($\tau_c/G_0 \approx 0.033$) and independent of the colloid volume fraction or the ionic strength of the system.[49]

Similar studies have been made on systems composed of charge-stabilized latex particles arranged onto an fcc lattice.[50−53] A critical stress where the viscosity drops by 1−3 orders of magnitude is found, signifying a major microstructural rearrangement,[50] with $\tau_c/G_0 \approx 0.04$ independent of colloid volume fraction.[53] Analogous flow behavior to what we observe here was also found for these colloidal systems, both at low stress where a defect-mediated flow of the ordered polycrystalline system was observed and at high stress where a low-viscosity plateau associated with an amorphous suspension was measured.[50−53] These similarities in behavior between colloidal and block copolymer materials clearly demonstrate that their viscoelastic response is dominated by the properties of the lattice and not by the nature of the elements from which the lattice is formed.

V. Conclusions

We have examined the rheological behavior of block copolymer materials possessing the bcc mesophase, including melts and concentrated solutions of S/I and S/EP diblock, triblock, and starblock systems. Using linear viscoelastic measurements and SAXS, we find that the lattice modulus G^0_{bcc} scales with the cube of the lattice spacing d_{110} and decreases as the reduced temperature $T_r \equiv T/T_{ODT}$ increases. At the ODT, each sphere per unit volume contributes $18k_BT$ to the modulus. We also measure a critical stress in each system which signifies shear-induced disordering of the bcc lattice. The critical strain τ_c/G^0_{bcc} is 0.038 for all block copolymer melts or highly concentrated solutions studied, a result which agrees well with values reported for other soft crystalline systems and even for certain metals. Its value decreases significantly in solutions

with concentrations approaching the lattice disordering concentration c_d, due to reduced interactions between neighboring micelles. The flow behavior exhibited by these ordered block copolymer systems is, therefore, directly related to the lattice in a manner quite analogous to that of other crystalline systems.

Acknowledgment. This work was supported by the National Science Foundation through the Princeton Center for Complex Materials (DMR-9400362 and -9809483) and a Graduate Fellowship (to J.M.S.). The authors thank Dr. Gary R. Marchand for providing most of the block copolymers, Professor William B. Russel for his many helpful suggestions, and Daniel A. Vega and Yueh-Lin Loo for assisting with several experiments.

References and Notes

(1) Holden, G., Legge, N. R., Quirk, R., Schroeder, H., Eds.; *Thermoplastic Elastomers*, 2nd ed.; Hanser/Gardner Publications: Cincinnati, OH, 1996.
(2) Larson, R. G. *Structure and Rheology of Complex Fluids*; Oxford University Press: New York, 1999.
(3) Colby, R. H. *Curr. Opin. Colloid Interface Sci.* **1996**, *1*, 454.
(4) Fredrickson, G. H.; Bates, F. S. *Annu. Rev. Mater. Sci.* **1996**, *26*, 501.
(5) Hamley, I. W. *The Physics of Block Copolymers*; Oxford University Press: Oxford, 1998.
(6) Kraus, G.; Naylor, F. E.; Rollman, K. W. *J. Polym. Sci., Part A-2* **1971**, *9*, 1839.
(7) Han, J. H.; Feng, D.; Choi-Feng, C.; Han, C. D. *Polymer* **1995**, *36*, 155.
(8) Hansen, P. J.; Williams, M. C. *Polym. Eng. Sci.* **1987**, *27*, 586.
(9) Chung, C. I.; Gale, J. C. *J. Polym. Sci., Polym. Phys. Ed.* **1976**, *14*, 1149.
(10) Holden, G. In *Block and Graft Copolymerization*; Ceresa, R. J., Ed.; John Wiley & Sons: London, 1974; Vol. 1, p 133.
(11) Henderson, C. P.; Williams, M. C. *J. Polym. Sci., Polym. Lett.* **1979**, *17*, 257.
(12) Watanabe, H.; Kotaka, T. *Polym. Eng. Rev.* **1984**, *4*, 73.
(13) Watanabe, H.; Kotaka, T. *Polym. J.* **1982**, *14*, 739.
(14) Hashimoto, T.; Shibayama, M.; Kawai, H.; Watanabe, H.; Kotaka, T. *Macromolecules* **1983**, *16*, 361.
(15) Spaans, R. D.; Williams, M. C. *Ind. Eng. Chem. Res.* **1995**, *34*, 3496.
(16) Doi, M.; Harden, J. L.; Ohta, T. *Macromolecules* **1993**, *26*, 4935.
(17) Ekong, E. A.; Jayaraman, K. *J. Rheol.* **1984**, *28*, 45.
(18) Kossuth, M. B.; Morse, D. C.; Bates, F. S. *J. Rheol.* **1999**, *43*, 167.
(19) Zhao, J.; Majumdar, B.; Schulz, M. F.; Bates, F. S.; Almdal, K.; Mortensen, K.; Hajduk, D. A.; Gruner, S. M. *Macromolecules* **1996**, *29*, 1204.
(20) Almdal, K.; Koppi, K. A.; Bates, F. S. *Macromolecules* **1993**, *26*, 4058.
(21) Koppi, K. A.; Tirrell, M.; Bates, F. S.; Almdal, K.; Mortensen, K. *J. Rheol.* **1994**, *38*, 999.
(22) Okamoto, S.; Saijo, K.; Hashimoto, T. *Macromolecules* **1994**, *27*, 3753.
(23) Daniel, C.; Hamley, I. W.; Mingvanish, W.; Booth, C. *Macromolecules* **2000**, *33*, 2163.
(24) Prud'homme, R. K.; Wu, G. W.; Schneider, D. K. *Langmuir* **1996**, *12*, 4651.
(25) Hamley, I. W.; Pople, J. A.; Booth, C.; Derici, L.; Imperor-Clerc, M.; Davidson, P. *Phys. Rev. E* **1998**, *58*, 7620.
(26) Eiser, E.; Molino, F.; Porte, G.; Diat, O. *Phys. Rev. E* **2000**, *61*, 6759.
(27) McConnell, G. A.; Lin, M. Y.; Gast, A. P. *Macromolecules* **1995**, *28*, 6754.
(28) Sebastian, J. M.; Lai, C.; Graessley, W. W.; Register, R. A.; Marchand, G. R. *Macromolecules* **2002**, *35*, 2700.
(29) Adams, J. L.; Graessley, W. W.; Register, R. A. *Macromolecules* **1994**, *27*, 6026.
(30) Adams, J. L.; Quiram, D. J.; Graessley, W. W.; Register, R. A.; Marchand, G. R. *Macromolecules* **1996**, *29*, 2929.
(31) Lai, C. Ph.D. Thesis, Princeton University, 1999.
(32) Adams, J. L.; Quiram, D. J.; Graessley, W. W.; Register, R. A.; Marchand, G. R. *Macromolecules* **1998**, *31*, 201.
(33) Pascoe, K. J. *An Introduction to the Properties of Engineering Materials*; Van Nostrand Reinhold: London, 1972.
(34) Buscall, R. *Colloid Surf. A* **1994**, *83*, 33.
(35) Buscall, R.; Goodwin, J. W.; Hawkins, M. W.; Ottewill, R. H. *J. Chem. Soc., Faraday Trans. 1* **1982**, *78*, 2889.
(36) Russel, W. B.; Saville, D. A.; Schowalter, W. R. *Colloidal Dispersions*; Cambridge University Press: Cambridge, 1989.
(37) Watanabe, H.; Kanaya, T.; Takahashi, Y. *Macromolecules* **2001**, *34*, 662.
(38) Witten, T. A.; Pincus, P. A. *Macromolecules* **1986**, *19*, 2509.
(39) Buitenhuis, J.; Förster, S. *J. Chem. Phys.* **1997**, *107*, 262.
(40) Kelarkis, A.; Mingvanish, W.; Daniel, C.; Li, H.; Havredaki, V.; Booth, C.; Hamley, I. W.; Ryan, A. J. *Phys. Chem. Chem. Phys.* **2000**, *2*, 2755.
(41) Frenkel, J. *Z. Phys.* **1926**, *37*, 572.
(42) Kelly, A.; Macmillan: N. H. *Strong Solids*, 3rd ed.; Clarendon Press: Oxford, 1986.
(43) Basinski, Z. S.; Duesbery, M. S.; Taylogy, R. In *Proceedings of the 2nd International Conference on the Strength of Metals and Alloys*; American Society of Metals: Materials Park, OH, 1970; p 118.
(44) Cannon, W. R.; Langdon, T. G. *J. Mater. Sci.* **1988**, *23*, 1.
(45) Hynes, A.; Doremus, R. *Crit. Rev. Solid State Mater. Sci.* **1996**, *21*, 129.
(46) Langdon, T. G. *Mater. Trans., JIM* **1996**, *37*, 359.
(47) Eiser, E.; Molino, F.; Porte, G.; Pithon, X. *Rheol. Acta* **2000**, *39*, 201.
(48) Eiser, E.; Molino, F.; Porte, G.; Diat, O. *Phys. Rev. E* **2000**, *61*, 759.
(49) Imhof, A.; Vanblaaderen, A.; Dhont, J. K. G. *Langmuir* **1994**, *10*, 3477.
(50) Chen, L. B.; Zukoski, C. F. *Phys. Rev. Lett.* **1990**, *65*, 44.
(51) Chen, L. B.; Zukoski, C. F. *J. Chem. Soc., Faraday Trans.* **1990**, *86*, 2629.
(52) Chen, L. B.; Zukoski, C. F.; Ackerson, B. J.; Hanley, H. J. M.; Straty, G. C.; Barker, J.; Glinka, C. J. *Phys. Rev. Lett.* **1992**, *69*, 688.
(53) Chen, L. B.; Chow, M. K.; Ackerson, B. J.; Zukoski, C. F. *Langmuir* **1994**, *10*, 2817.

MA011523+